Mausam, (1994), **45**, 1, 1–6

551.468.6

The modelling study of flow in Vasishta Godavari estuary

A. D. RAO, S. CHAMARTHI and P. C. SINHA

Centre for Atmospheric Sciences, I.I.T., New Delhi

(*Received 21 July 1993*)

सार –– गोदावरी मुहाने की सहायक धारा वशिष्ट, बंगाल की खाड़ी में अन्तरवेदी नामक स्थान पर गिरती है । गोदावरी के मुहाने पर पाई जाने वाली अवस्थाएं, मौसम के अनुसार परिवर्तनशील ताजे जलस्त्राव और अर्द्ध-दिवसीय ज्वार-भाटे से सम्बद्ध खाड़ी के खारे जल के आपस में मिलने के कारण अभिलक्षित होती है । उसकी विशिष्टताओं का वर्णन इसमें किया गया है। जल के प्रवाह और खारेपन का अनुकरण करने के लिए एक संख्यात्मक मॉडल का अनुप्रयोग किया गया है । इसका उल्लेख वैज्ञानिक साहित्य में भी उपलब्ध है। प्रक्षोभ क्लोजर स्कीम के प्रयोग द्वारा मॉडल से व्युत्पन्न सैद्धान्तिक परिणामों की तुलना में मानसून और मानसूनोत्तर ऋतुओं के दौरान लिए गए प्रेक्षणों का प्रयोग किया गया है ।

ABSTRACT. The Vasishta branch of the Godavari estuary opens into the Bay of Bengal at Antarvedi. Conditions in the estuary are characterized by a seasonally varying fresh water discharge and salt water intrusion from the Bay resulting from the flow associated with the semi-diurnal tide. A numerical model is applied to simulate the flow and salinity structures which have also been documented in the literature. The observations during monsoon and post-monsoon seasons are used in a comparison with the theoretical results which are derived from a model in which turbulence closure scheme is used.

Key words — Godavari estuary, Freshwater discharge, Semi-diurnal tide, Numerical model, Estuarine circulation.

1. Introduction

The distance of inland penetration of saline water in the estuary varies with the relative strength of the freshwater flow from upstream and the tidal flow from adjacent sea. Additional variability will occur in response to different rates of freshwater discharge into the estuary. As the inland penetration of saline water has a significant effect on the water resources in the estuarine region, it is of practical relevance to consider the development and application of a suitable numerical model in the region in order to study the circulation in the region.

The processes involving the interaction between freshwater flow and tidal currents are complex and lead to different types of estuary circulations (Dyer 1973, Officer 1976). If the river discharge dominates over a relatively weak tidal flow, freshwater flows out of estuary through a surface layer which results in a stratified estuary. In the other extreme, when tidal flow dominates over freshwater flow, results in a well mixed condition with practically negligible density gradients. Thus, in any numerical model of estuarine circulation, it is apparent that a practical requirement is that the vertical mixing mechanisms be correctly represented. Recognition of this aspect led several authors (Beardsley and Hart 1978, Zhang *et al.* 1987) to study interactive effect between estuary outflow and the adjacent coastal dynamics.

Ramana *et al.* (1989) studied the distribution of salinity and current in the Vasishta branch of Godavari estuary associated to the freshwater discharge and tides in 3 representative months. Simultaneous hourly observations of salinity and current over 18 hours were made at each of 3 selected stations (Fig. 1). The duration of observations time (18 hrs) is so chosen that it would cover a full cycle of a semi-diurnal tide (12.4 hrs). The stations are located along the channel where maximum depths were encountered across the channel. Salinities and currents were measured at 2 m depth intervals from surface to 1 m above the bottom to obtain vertical profiles. According to the observations, it is stated that in July, when the river discharge is very high, the estuary behaves some characteristics of a salt wedge type while during February when the discharge is minimum, the estuary becomes a well mixed one.

Johns and Oguz (1990) developed a numerical model for the exchange of water between the Black Sea and the Marmara Sea through the Bosphorous. It is a multi-level, two dimensional, channel model. An essential part of their modelling procedure is the use of a turbulence energy equation in a scheme of turbulence parameterization. They added a transport equation to the system which describes how salinity is advected and diffused through the channel. The form of the boundary conditions applied on the salinity at the ends of the channel are based on the flow in the channel. They have

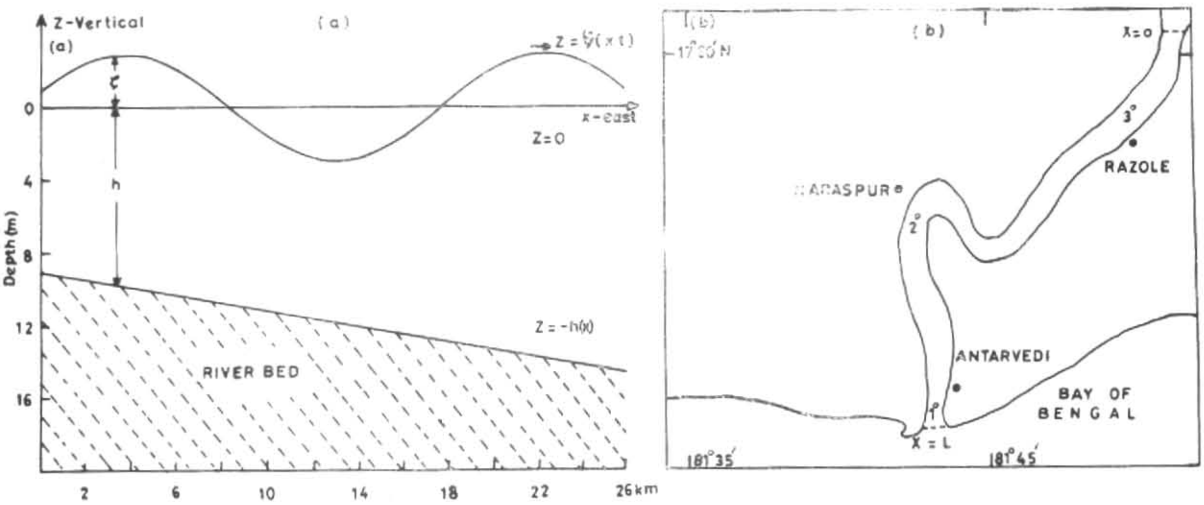

Figs. 1(a & b). (a) Coordinate representation of the Vasishta Godavari estuary, and (b) Topography of the estuary

not considered the tide effect in the Bosphorous strait. It is also noted in their formulation that the density of the sea water is determined by only salinity.

In the present work, the basic formulation is based upon the multi-level numerical model described above (Johns and Oguz 1990) with proper prescription of flow conditions at the ends of the model estuary. Based on tide observations of Ramana *et al.* (1989), we have included the tide effect in the form of a progressive wave at the seaward end of the estuary. Since the estuarine circulation is mainly dependent on the density distribution, we have considered the density as a function of both salinity and temperature. The salinities and currents were obtained over a tidal cycle for July and January representative months of high and low freshwater flow conditions respectively.

2. Formulation of model

We briefly describe the model equations (Johns and Oguz 1990) used for the present study with a system of rectangular cartesian coordinates in which the origin 0, is within the equilibrium level of the water surface. $0x$ points seaward from the landward end of the estuary considered at $x=0$, the seaward end is denoted by $x=L$ and $0z$ is directed vertically upwards from $z=0$ [Figs. 1 (a & b)]. The displaced position of the water surface is given by $z=\zeta\ (x,\ t)$ and the position of the bed of the estuary is at $z=-h(x)$. The breadth of the estuary at position x is denoted by $b\,(x)$. The equation of continuity and the equation expressing the horizontal momentum balance in the estuary are of the form

$$b\,\frac{\partial H}{dt}+\frac{\partial}{\partial x}\,(bH\bar{u})=0 \tag{1}$$

$$\frac{\partial}{\partial t}\,(bu)+\frac{\partial}{\partial x}\,(bu^2)+\frac{\partial}{\partial z}\,(buw)=-gb\,\frac{\partial\zeta}{\partial x}-\frac{b}{\rho_0}\int_z^{\zeta}\frac{\partial}{\partial x}\,(g\rho)dz+\frac{\partial}{\partial z}\left[K_M\frac{\partial}{\partial z}\,(bu)\right] \tag{2}$$

where, $(u,\ w)$, components of fluid velocity; ρ, the fluid density; ρ_0, a constant reference density; K_M, a diffusion coefficient for vertical momentum exchange by turbulent processes; and H, the total depth $\zeta+h$. $\bar{u}$ is the depth averaged velocity given by

$$\bar{u}=\frac{1}{H}\int_{-h}^{\zeta}u dz \tag{3}$$

The density is determined by the local temperature and salinity by a linear equation of state in which

$$\rho=\rho_0\,(1-\alpha T+\delta S) \tag{4}$$

where, the constants α and δ are taken as $2.0\times10^{-4}/°C$ and 7.5×10^{-4}/ppt respectively.

The temperature and salinity are determined from a transport equation having the form

$$\frac{\partial}{\partial t}\,(bT)+\frac{\partial}{\partial x}\,(buT)+\frac{\partial}{\partial z}\,(bwT)=\frac{\partial}{\partial z}\left[K_T\,\frac{\partial}{\partial z}\,(bT)\right] \tag{5}$$

$$\frac{\partial}{\partial t}\,(bS)+\frac{\partial}{\partial x}\,(buS)+\frac{\partial}{\partial z}\,(bwS)=\frac{\partial}{\partial z}\left[K_S\,\frac{\partial}{\partial z}\,(bS)\right] \tag{6}$$

when K_T and K_S are vertical diffusion coefficients for thermal exchange and salinity exchange.

The parameterization of the turbulent processes is completed by the application of a transport equation for the Reynolds-averaged turbulence energy density, E. This has the form

$$\frac{\partial}{\partial t}\,(bE)+\frac{\partial}{\partial x}\,(buE)+\frac{\partial}{\partial z}\,(bwE)=bK_M\left(\frac{\partial u}{\partial z}\right)^2+\frac{g}{\rho_0}\,bK_D\,\frac{\partial\rho}{\partial z}+\frac{\partial}{\partial z}\left[K_E\,\frac{\partial}{\partial z}\,(bE)\right]-b\,\epsilon \tag{7}$$

where, K_D and K_E are respectively diffusion coefficients for the vertical exchange of density and turbulence energy. On the right hand side of Eqn. (7), the first term represents a production of turbulence energy consequent upon there being a vertical shear in the Reynolds-averaged flow. For $\left(\frac{\partial \rho}{\partial z}\right)<0$, the second term represents a sink of turbulence energy resulting from the presence of a stable density stratification. The third one represents a vertical diffusion of turbulence energy with an eddy coefficient, K_E. The last term, involving ϵ, simulates the dissipation of turbulence energy. We have not considered terms representing production of turbulence energy associated with the action of normal eddy stresses and horizontal redistribution of turbulence energy by the turbulence itself. These two terms are neglected in the present study as there is no evidence of a tendency for the formation of an internal hydraulic jump.

In the present study, we prescribe that the diffusion coefficients are equal in value for all transfer processes and write

$$K_M = K_T = K_s = K_D = K_E = K \tag{8}$$

$$K = c^{1/4}\, l E^{1/2} \tag{9}$$

$$\epsilon = \frac{c^{3/4}\, E^{3/2}}{l_D} \tag{10}$$

where, l is vertical mixing length scale, l_D is a dissipation length scale and c an empirical constant recommended by Launder and Spalding (1972) as 0.08. At the first time step of integration of the model, the eddy coefficient, K, is set equal to a small value of 0.0001 and this is used to solve the governing equations. In the subsequent time steps, the value is calculated with Eqn. (9). The form used for the length scale is a unique feature of the present work and has been chosen so as to simulate a best agreement with the reported observations (Ramana *et al.* 1989).

A basic length scale, l_0, is defined by

$$l_0 = k\,(z + h + z_0)\,\exp\left[-\left(\frac{z+h}{H}\right)^{\gamma}\right] \tag{11}$$

where, k and z_0 are respectively Von Karman's constant (taken as 0.4) and bottom roughness. In terms of this, we write

$$l = l_0 \exp\left[\frac{-1}{4}\,\beta\left(\frac{h_0}{h}\right)^2\left(\frac{z+h}{H}\right)\right] \tag{12}$$

where β, γ are constants and h_0 is a constant reference depth, thus as $z \to -h$, $l \to kz_0$. A dissipation length scale, l_D, defined by

$$l_D = l_0 \exp\left[\frac{3}{4}\,\beta\left(\frac{h_0}{h}\right)^2\left(\frac{z+h}{H}\right)\right] \tag{13}$$

the availability of the disposable parameters β and γ enables variation in the mixing length and dissipation length scales near the free surface at $z=\zeta$. Although, such a parameterization is arbitrary in form, it is found that this is important in the successful simulation of the flow conditions observed in the Vasishta Godavari estuary. The boundary conditions at $x=0$ and $x=L$ are given by

$$\bar{u} + \left(\frac{g}{h}\right)^{\frac{1}{2}} \zeta = 2u_0 \tag{14}$$

$$\bar{u} - \left(\frac{g}{h}\right)^{\frac{1}{2}} \zeta = -2u_L \sin(\sigma t) \tag{15}$$

where, u_0, a constant velocity that determines the strength of the freshwater flow; u_L, also a constant velocity the value of which will be chosen so as to produce the correct amplitude for the semi-diurnal tide; σ, the corresponding radian frequency (taken as $1.405 \times 10^{-4} s^{-1}$).

The numerical solution of these equations is obtained by integrating ahead in time with boundary forcing given by Eqns. (14) and (15) until a complete oscillatory response is attained. This response then forms the basis to study the flow conditions in the estuary. Evaluations are made of salinity and current distribution along the channel and these are compared with observational data. Since the $M2$ tide is more dominant in the Bay of Bengal, we consider this tide to study its effect in the estuary. Its corresponding time period (T) is 12.4 hrs.

3. Method of numerical solution

The equations described in the above section are solved on a finite difference grid in the x—σ domain. We define;

$$\left.\begin{aligned} x &= (i-1)\,\triangle x,\; i=1,2,\ldots,m,\; \triangle x = L/(m-1) \\ \sigma &= (j-1)\,\triangle\sigma,\; j=1,2,\ldots,n,\; \triangle\sigma = 1/(n-1) \end{aligned}\right\} \tag{16}$$

$$t = p\,\triangle t, \quad p = 0, 1, 2, \ldots \tag{17}$$

The finite sequence of x values consists of points of two distinct types. Odd values of i correspond to positions at which we evaluate the dependent variables ζ, S and T. Even values of i correspond to positions at which we evaluate the dependent variables u and E. We choose m to be odd so that the end points of the computational domain correspond to ζ-points. The formal descretization of Eqns. (1), (2) and (5)-(7) follow those described by Johns and Qguz (1990) and Johns (1978). It is, however, worthwhile to mention here the method of implementing Eqns. (14) and (15) as this is crucial to the solution procedure in the present study.

We use a conventional subscript notation to reference grid-point values of the dependent variables and denote the time-level by a superscript. In practice, we apply Eqn. (15) at $x=L-\triangle x$ which is a u-point. Furthermore, we evaluate the depth-averaged velocity at the lower time-level, thus introducing an error $0(\triangle t)$. Therefore, we write Eqn. (15) as

$$\bar{u}^{\,p}_{m-1} - \frac{1}{2}\left[\frac{g}{h_{m-1}}\right]^{\frac{1}{2}}\left[\zeta^{p+1}_{m} + \zeta^{p+1}_{m-2}\right] = -2\,u_L \sin\left(\frac{2\pi t}{T}\right) \tag{18}$$

Because the elevation, ζ, is not calculated at $i=m-1$, we have applied its value thereby averaging of its value at the two adjacent ζ-points.

Eqn. (18) then leads to

$$\zeta^{p+1}_{m} = -\zeta^{p+1}_{m-2} + 2\left[\frac{h_{m-1}}{g}\right]^{1/2}\left[2u_L \sin\left(\frac{2\pi t}{T}\right) - \bar{u}^{\,p}_{m-1}\right] \tag{19}$$

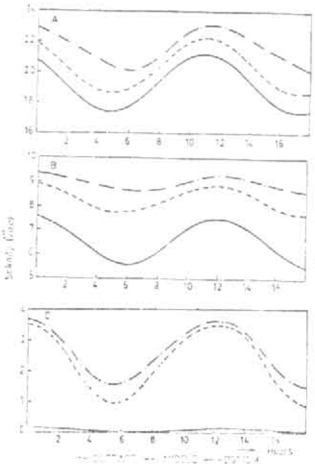

Figs. 2(a-c). Salinity variation over a tidal cycle in July at stations 1, 2 and 3

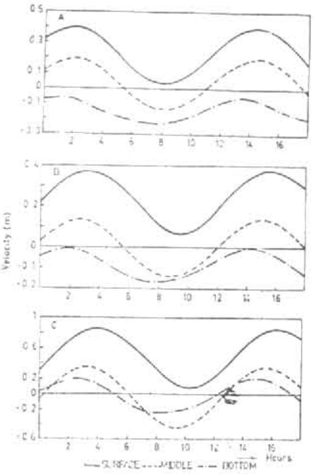

Figs. 3(a-c). Velocity profiles over a tidal cycle in July at stations 1, 2 and 3

Thus, Eqn. (19) yields a method of updating ζ at $x=L$ which utilizes an already-known interior updated value of ζ together with the depth-averaged velocity derived from the previous time-step.

In a similar manner, Eqn. (14) gives

$$\zeta_1^{p+1} = -\zeta_3^{p+1} + 2\left[\frac{h_2}{g}\right]^{\frac{1}{2}}\left[2u_0 - \bar{u}_2^{\,p}\right] \quad (20)$$

We then integrate the governing Eqns. forward in time and with steady-state forcing, continue until the initial transient response is both radiated out of the analysis region and is essentially dissipated by the action of friction. The remaining steady state fields will then represent the response to the prescribed steady-state forcing.

4. Numerical experiments

The length of the estuary in the model is restricted to 26 km as the tidal influence is observed up to this distance from the mouth of the estuary. Based upon topographical and bathymetric information (Ramana *et al.* 1989), the breadth varies between 500 m and 900 m and the mean depth of the estuary varies between 9 m and 15 m [Fig. 1 (a)]. The selection of $m=29$ in the formulation implies that the horizontal grid-distance is 900 m. The prescription of 21 computational levels in the vertical implies a vertical grid spacing varies from 0.4 m in the shallow region to 2 m in the region of maximum depth. With our scheme of descretization, the attainment of computational stability in the solution procedure is secured by taking $\triangle t=60$s.

Results from two numerical experiments are described in this section that correspond to the freshwater flow condition in the estuary during the months July and January. Detailed observational data on the dynamical and salinity structure for these months are given by Ramana *et al.* (1989). Our main purpose here is to assess the effectiveness of the numerical modelling procedure by comparing the computed salinity and tidal current distributions with their observational counterparts. Conclusions will then be drawn on the corresponding structure of the density-controlled circulation.

In both experiments, the turbulent mixing parameters β and γ appearing in Eqns. (11), (12) and (13) are set equal to optional values of 23 and 24 respectively; the constant depth h_0 is set equal to 10 m. The roughness length z_0 is set to 1 cm. After performing several numerical experiments, these settings are chosen based on simulation of best mixing conditions due to production of vertical shear in the estuary. We compared our model simulations with the observations available at 3 different stations [Fig. 1(b)] along the river. Station 1 and 3 are situated near the mouth of the estuary (seaward end) and the upstream end respectively while station 2 located in between stations 1 and 3. The distance between station 1 and 3 is 24 km.

In the first experiment, temperature and salinity boundary conditions for July are based on observations (Ramana *et al.* 1989) which correspond to $T_0=26.5°$C, $T_L=27.5°$ C, $S_0=0$ ppt, $S_L=29$ ppt. This implies that at $x=0$ in the model estuary, the inflow is assumed to be of freshwater. The freshwater and tidal flow conditions in the estuary are fixed by taking $u_0=0.08$m s^{-1}, $u_L=0.21$ms^{-1}. With this parameter setting, we find that the mean volume flux of water through the model estuary is about 100m^3 s^{-1} consistent with the reported value in Ramana *et al.* (1989).

The salinity variation with depth over a tidal cycle is given in Figs. 2 (a-c) at stations 1-3 respectively. The maximum surface salinity at the mouth of the estuary is about 21 ppt [Fig. 2(a)]. Except at station 2 [Fig. 2(b)], the salinity varies about 3 ppt between high and low tide. At station 3 which is almost about 20 km from station 1, the estuary is almost filled with freshwater [Fig. 2(c)]. It is noticed from the simulations that at the bottom (1.0 m above the estuary bottom) salt water has intruded

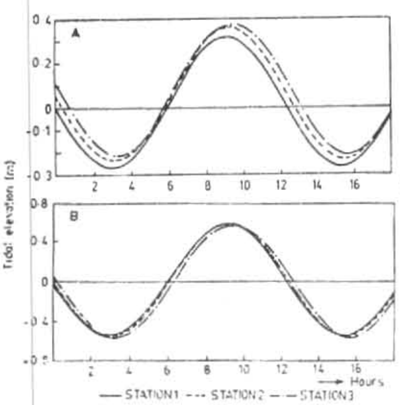

Figs. 4 (a & b). Tidal elevation during a tidal cycle for July and January

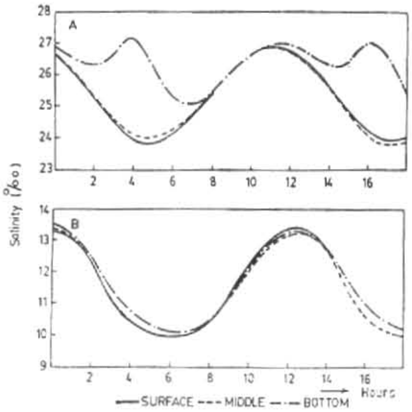

Figs. 5 (a & b). Salinity variation over a tidal cycle in January at stations 1 and 3

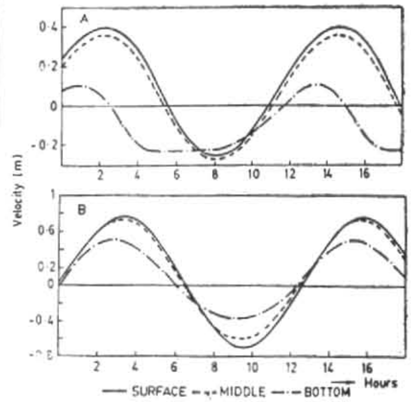

Figs. 6 (a & b). Velocity profiles over a tidal cycle in January at stations 1 and 3

more than 24 km upstream along the estuary producing salinities near $x=0$ of order 4 ppt. This is inspite of a relatively strong seaward flow of freshwater which tend to oppose the inland penetration of saline water.

Figs. 3 (a-c) provide velocities over a tidal cycle at different depths and at different stations 1-3 respectively. As the freshwater discharge is high in July, the seaward directed current increases as we approach towards landward end of model river from its mouth. It attains a maximum velocity of $0.85 \mathrm{m\,s^{-1}}$ corresponding to the low tide phase and a minimum of $0.1 \mathrm{m\,s^{-1}}$ at the time of high tide. Similarly, maximum landward directed current is about $0.45 \mathrm{m\,s^{-1}}$ which occurs at the time of high tide [Fig. 3 (c)]. Fig. 4 (a) depicts tidal elevation during a tidal cycle for July month. It is noticed that the tide range is about 0.7 m. The tide input to the model (depends on the value of u_L) is consistent with the reported value (Ramana *et al.* 1989). It is also noticed from Figs. 3 and 4(a) that during low tide phase the ebb currents (positive velocity) dominate at the surface and intermediate levels. Weak flood currents are however, noticed at the bottom during this period at stations 1 and 2. At the surface, the maximum ebb currents are occurring almost at the time of low tide. While at the intermediate level, the change in the direction of currents from ebb to flood takes place about 2 hrs after the occurrence of the low tide. These simulations clearly show that the sea water penetrated into the estuary in the form of a thin saline wedge across the mouth. The model simulations of the flow and salinity structure for the month of July are qualitatively in agreement with observations (Ramana *et al.* 1989).

The second experiment described here relates to the estuary flow during January when there is a negligible freshwater inflow. Based on tidal and freshwater flow conditions, we choose $u_0=0.035 \mathrm{m\,s^{-1}}$ and $u_L=0.4 \mathrm{m\,s^{-1}}$. Accordingly, with a reduced value of u_0, there will be an increased inland penetration of saline water from the Bay and for a model estuary with a fixed length of 26 km, there must be a change in the boundary condition on S at $x=0$ which should be consistent with the observations. Keeping this in view, we therefore take $S_0=10$ ppt in contrast with $S_0=0$ in the previous experiment. All other parameters remain unchanged. With this parameter setting, the mean volume flow through the estuary is negligible.

Fig. 4(b) gives the tidal elevation for January. The tide range is high compared to Fig. 4(a) and is about 1.2 m. The salinity variations over a tidal period for January are simulated at station 1 [Fig. 5(a)] and at station3[Fig. 5(b)]. In January, the effect of tide is noticed even at station 3 [Fig. 5(b)], situated about 24 km upstream from the mouth of the estuary. At station 3, the salinity of the surface water reaches about 13.5 ppt. We confirm from Fig. 5, the entire estuary is well mixed and salinity difference from surface to bottom is quite small. Figs. 6 (a & b) show velocity variation over a tidal cycle at stations 1 and 3 for January. An important feature in the simulation is that when there is no freshwater discharge, even the surface layers of the estuary are dominated by the tide even at the time of high tide (Fig. 6). As a result, the surface currents change sign depending on the tide conditions. This is in contrast with the simulation for July (Fig. 3), where due to freshwater discharge ebb currents dominate at all three stations over a tidal cycle. We also note that the effect of bottom friction is reducing the current near the bed of the estuary. In January, strong flood currents (Fig. 6) are encountered at all levels compared to the simultations for July (Fig. 3). In January, all the stations in the estuary, in general, represent well mixed conditions. These conditions are consistent with the observations available (Ramana *et al.* 1989).

5. Conclusions

Numerical experiments have been performed to simulate the flow and salinity structure in Vasishta branch of the Godavari estuary. Using a multi-level numerical model, the tide and the turbulent mixing parameters have been chosen so as to yield the best overall agreement with observational data reported by Ramana *et al.* (1989). With the corresponding parameters setting, a study has been made of the salinity and current structure along the estuary during both the high and the low freshwater discharge conditions. A qualitative comparison between the model results and observation provides a substantial support to the fact that in July the estuary exhibits characteristics akin to a salt wedge type, while in February the estuary becomes a well mixed one.

References

Beardsley, R.C. and Hart, J., 1978, "A simple theoretical model for the flow of an estuary onto a continental shelf", *J. Geophys. Res.*, **83**, 873.

Dyer, K.R., 1973, Estuaries : A physical introduction, John Wiley, London, 140 pp.

Johns, B., 1978, "The modelling of the tidal flow in a channel using a turbulence energy closure scheme", *J. Phys. Oceanogr.*, **8**, 1042-1049.

Johns, B. and Oguz, T., 1990, "The modelling of the flow of water through the Bosphorus", *Dyn. Atmos. Oceans*, **14**, 229.

Launder, B.E. and Spalding, D.B., 1972, Mathematical models of turbulence, Academic Press, New York.

Officer, C.B., 1976, Physical oceanography of estuaries (and associated coastal waters), John Wiley, New York, 465 pp.

Ramana, Y.V., Ranga Rao, V. and Reddy, B.S.R., 1989, "Diurnal variation in salinity and currents in Vasishta Godavari estuary, east coast of India", *Indian J. Mar. Sci.*, **18**, 54.

Zhang, Q. H., Janowitz, G.S. and Pietrafesa, L.J., 1987, "The interaction of estuarine and shelf waters : A model and applications", *J. Phys. Oceanogr.*, **17**, 455.